

5 MECHANISMS AND DYNAMIC SYSTEMS

5.1 Optimal Counterweight Balancing of Robot Arms Using Multicriteria Approach

J. Koski, A. Osyczka

5.1.1 Introduction

The increasing application of industrial robots in different fields of technology augments the demand for further improvement of their performance. Energy consumption and working accuracy especially are becoming more and more important in assessing the efficiency of a robot. One way to improve these factors is the proper balancing of a robot manipulator. There are two main methods of balancing a robot manipulator: 1) by spring mechanisms or 2) by counterweights [1,2]. The problem of the optimum design of a robot spring balancing mechanism is discussed in Chapter 5.2. In this chapter, counterweight balancing of robot arms is the subject of investigation.

Counterweight balancing is often used for establishing better mass distributions of mechanisms, and some approaches to the optimum design of different kinds of mechanisms have been discussed in the literature [3,4,5]. Since the balancing of a robot manipulator involves the minimization of driving forces or torques as well as the support reactions at joints, it seems reasonable to apply the multicriteria approach. Using this approach, an optimization model based on the rigid-body dynamics of robot arms is presented. The solution of the multicriteria optimization model provides the designer with a set of Pareto-optimal solutions which enables him to make the right decision in a conflicting situation.

5.1.2 Kinetic Model of a Robot Arm

Two alternative approaches are generally used in deriving the equations of motion for robot manipulators. These are the Lagrangian and the Newton-Euler approaches. By using angular coordinates for the PUMA-560 robot, schematically shown in Fig. 5.1/1, it is possible to calculate the generalized torques at each joint applying the following equation:

$$M_{ti} = \frac{d}{dt} \left(\frac{\partial L}{\partial \dot{\theta}_i} \right) - \frac{\partial L}{\partial \theta_i}, \quad (5.1-1)$$

where θ_i is the rotation at joint i and $\dot{\theta}_i$ is the corresponding angular velocity. The term

$$L = T - V \quad (5.1-2)$$

represents the Lagrangian function of the mechanical system. Here, T is the total kinetic energy of the system and V is the total potential energy. The application of (5.1-1) to a fully articulated robot arm results in the following nonlinear second-order system of differential equations

$$A\ddot{\theta} + B\dot{\theta}^2 + c - m = 0, \quad (5.1-3)$$

Here, the vector of angular accelerations is given by

$$\ddot{\theta} = (\ddot{\theta}_1, \ddot{\theta}_2, \dots, \ddot{\theta}_N)^T, \quad (5.1-4)$$

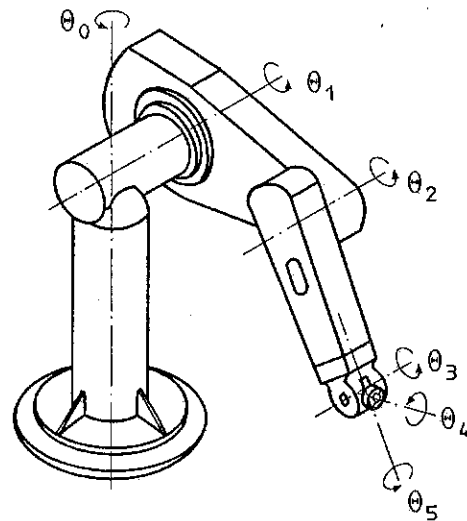


Fig. 5.1/1. PUMA-560 robot and schematic representation of coordinate angles θ_i

and the vector of squared angular velocities by

$$\dot{\theta}^2 = (\dot{\theta}_1 \dot{\theta}_1, \dot{\theta}_1 \dot{\theta}_2, \dots, \dot{\theta}_1 \dot{\theta}_N \mid \dot{\theta}_2 \dot{\theta}_1, \dot{\theta}_2 \dot{\theta}_2, \dots, \dot{\theta}_2 \dot{\theta}_N \mid \dots \dot{\theta}_k \dot{\theta}_1, \dot{\theta}_k \dot{\theta}_2, \dots, \dot{\theta}_k \dot{\theta}_N \mid \dots \dot{\theta}_N \dot{\theta}_1, \dot{\theta}_N \dot{\theta}_2, \dots, \dot{\theta}_N \dot{\theta}_N)^T, \quad (5.1-5)$$

where N is the number of joints. The corresponding matrices are

$$A = \begin{bmatrix} D_{11} & D_{12} & \dots & D_{1N} \\ D_{21} & D_{22} & \dots & D_{2N} \\ \vdots & \vdots & \ddots & \vdots \\ D_{N1} & D_{N2} & \dots & D_{NN} \end{bmatrix}$$

and

$$B = \begin{bmatrix} D_{11}^1 & D_{12}^1 & \dots & D_{1N}^1 & \mid & D_{11}^2 & D_{12}^2 & \dots & D_{1N}^2 & \mid & D_{11}^N & D_{12}^N & \dots & D_{1N}^N \\ D_{21}^1 & D_{22}^1 & \dots & D_{2N}^1 & \mid & D_{21}^2 & D_{22}^2 & \dots & D_{2N}^2 & \mid & D_{21}^N & D_{22}^N & \dots & D_{2N}^N \\ \vdots & \vdots & \ddots & \vdots & \mid & \vdots & \vdots & \ddots & \vdots & \mid & \vdots & \vdots & \ddots & \vdots \\ D_{N1}^1 & D_{N2}^1 & \dots & D_{NN}^1 & \mid & D_{N1}^2 & D_{N2}^2 & \dots & D_{NN}^2 & \mid & D_{N1}^N & D_{N2}^N & \dots & D_{NN}^N \end{bmatrix}, \quad (5.1-6)$$

where it is assumed that each joint has one degree of freedom. The elements of matrix A are the inertia terms, and the elements of matrix B represent the centripetal and Coriolis terms. All these terms depend on the position of the arm, i.e. $D_{ij} = D_{ij}(\theta_i)$. Vector $c = (D_1, D_2, \dots, D_N)^T$ includes the gravitational terms D_i , and m is the vector of torques. Kinetic equations (5.1-3) represent the rigid-body motion of the arm, and they are geometrically nonlinear because of large rotations θ_i .

The manipulator is an isostatic structure, and thus it is possible to get explicit expressions for all forces and moments in the system. The friction in the joints as well as the flexibility of the arm are not included in the following design model. For the application of opti-

mization methods, a two-member robot arm, which corresponds to the two arms of PUMA-560 robot in a plane motion, is considered. This arm is assumed to move in the xy -plane only (corresponding angular coordinates θ_i are shown in Fig. 5.1/2). The masses of the members are m_1 and m_2 . They are located as point masses at distances e_1 and e_2 from the joints. The external load is represented by the point mass m_3 . In the sequel, only the counterweight masses m_4 and m_5 as well as their distances from the joints x_1 and x_2 are treated as design variables, whereas all the other quantities are fixed.

The torques of this two-member robot are obtained from the Eq. (5.1-1) and are expressed as follows:

$$\begin{aligned} M_{t1} &= D_{11}\ddot{\theta}_1 + D_{12}\ddot{\theta}_2 + D_{11}^1\dot{\theta}_1^2 + D_{12}^2\dot{\theta}_2^2 + (D_{12}^1 + D_{11}^2)\dot{\theta}_1\dot{\theta}_2 + D_1, \\ M_{t2} &= D_{21}\ddot{\theta}_1 + D_{22}\ddot{\theta}_2 + D_{21}^1\dot{\theta}_1^2 + D_{22}^2\dot{\theta}_2^2 + (D_{22}^1 + D_{21}^2)\dot{\theta}_1\dot{\theta}_2 + D_2. \end{aligned} \quad (5.1-7)$$

The terms appearing in these equations are defined in the Appendix.

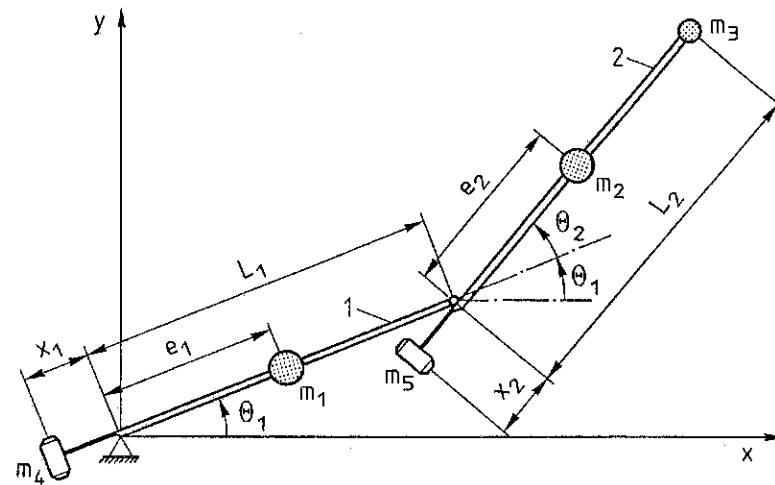


Fig. 5.1/2. Mechanical model of a robot arm for optimization

In addition to the torques, the joint forces are considered in the optimization process. In the present application, the most convenient way of solving them is to use the force equilibrium conditions in both coordinate directions x and y . For this purpose, the free-body diagrams of both members have been depicted in Fig. 5.1/3. The positive directions in the figure are associated with the global xy -axes, and the positive rotation direction is counterclockwise. By computing the accelerations from the well-known kinematic equation

$$\mathbf{a}_p = \mathbf{a}_Q + \boldsymbol{\alpha} \times \mathbf{r}_{p/Q} + \boldsymbol{\omega} \times (\boldsymbol{\omega} \times \mathbf{r}_{p/Q}), \quad (5.1-8)$$

analytic expressions for \mathbf{a}_i ($i=1, \dots, 5$) can be obtained. Here, \mathbf{a}_Q is the acceleration vector of the comparison point, $\boldsymbol{\alpha}$ the angular acceleration vector of the member, $\mathbf{r}_{p/Q}$ the position vector from point P to point Q along the member, and $\boldsymbol{\omega}$ the angular velocity of the member. For member 1 point Q is the support point and $\boldsymbol{\alpha} = (0, 0, \ddot{\theta}_1)^T$, $\boldsymbol{\omega} = (0, 0, \dot{\theta}_1)^T$. For member 2 point Q is at the joint and $\boldsymbol{\alpha} = (0, 0, \ddot{\theta}_0)^T$, $\boldsymbol{\omega} = (0, 0, \dot{\theta}_0)^T$ where $\theta_0 = \theta_1 + \theta_2$. Vector $\mathbf{r}_{p/Q}$ depends on the 5 selected calculation points. Here, the detailed expressions for the accelerations are presented separately, and they also appear as a part of the terms in (5.1-7). The corresponding inertia forces $m_i \mathbf{a}_i$ ($i=1, \dots, 5$) and the moments $J_j \alpha_j$, ($j=1, 2$) with the complete free-body diagrams are shown in Fig. 5.1/3.

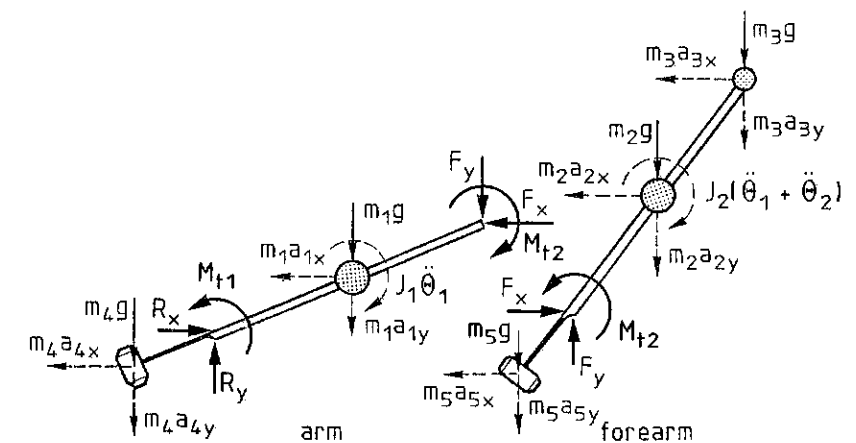


Fig. 5.1/3. Free-body diagrams of robot arms

The accelerations of the points at which the point masses are located have the following explicit expressions:

$$\begin{aligned}
 \mathbf{a}_1 &= \ddot{\theta}_1 \mathbf{e}_1 \begin{bmatrix} -\sin \theta_1 \\ \cos \theta_1 \end{bmatrix} - \dot{\theta}_1^2 \mathbf{e}_1 \begin{bmatrix} \cos \theta_1 \\ \sin \theta_1 \end{bmatrix}, \\
 \mathbf{a}_2 &= \ddot{\theta}_1 L_1 \begin{bmatrix} -\sin \theta_1 \\ \cos \theta_1 \end{bmatrix} - \dot{\theta}_1^2 L_1 \begin{bmatrix} \cos \theta_1 \\ \sin \theta_1 \end{bmatrix} + \mathbf{e}_2 \ddot{\theta}_0 \begin{bmatrix} -\sin \theta_0 \\ \cos \theta_0 \end{bmatrix} + \\
 &\quad \mathbf{e}_2 \dot{\theta}_0^2 \begin{bmatrix} -\cos \theta_0 \\ -\sin \theta_0 \end{bmatrix}, \\
 \mathbf{a}_3 &= \ddot{\theta}_1 L_1 \begin{bmatrix} -\sin \theta_1 \\ \cos \theta_1 \end{bmatrix} - \dot{\theta}_1^2 L_1 \begin{bmatrix} \cos \theta_1 \\ \sin \theta_1 \end{bmatrix} + L_2 \ddot{\theta}_0 \begin{bmatrix} -\sin \theta_0 \\ \cos \theta_0 \end{bmatrix} + \\
 &\quad + L_2 \dot{\theta}_0^2 \begin{bmatrix} -\cos \theta_0 \\ -\sin \theta_0 \end{bmatrix}, \\
 \mathbf{a}_4 &= \ddot{\theta}_1 x_1 \begin{bmatrix} \sin \theta_1 \\ -\cos \theta_1 \end{bmatrix} + \dot{\theta}_1^2 x_1 \begin{bmatrix} \cos \theta_1 \\ \sin \theta_1 \end{bmatrix}, \\
 \mathbf{a}_5 &= \ddot{\theta}_1 L_1 \begin{bmatrix} -\sin \theta_1 \\ \cos \theta_1 \end{bmatrix} - \dot{\theta}_1^2 L_1 \begin{bmatrix} \cos \theta_1 \\ \sin \theta_1 \end{bmatrix} + x_2 \ddot{\theta}_0 \begin{bmatrix} \sin \theta_0 \\ -\cos \theta_0 \end{bmatrix} + \\
 &\quad + x_2 \dot{\theta}_0^2 \begin{bmatrix} \cos \theta_0 \\ \sin \theta_0 \end{bmatrix}.
 \end{aligned} \tag{5.1-9}$$

Here again the notations $\theta_0 = \theta_1 + \theta_2$, $\dot{\theta}_0 = \dot{\theta}_1 + \dot{\theta}_2$ and $\ddot{\theta}_0 = \ddot{\theta}_1 + \ddot{\theta}_2$ have been used. By applying the force equilibrium conditions in the coordinate directions, the following joint reactions (see Fig. 5.1/3)

$$\begin{aligned}
 R_{2x} &= m_2 a_{2x} + m_3 a_{3x} + m_5 a_{5x}, \\
 R_{2y} &= m_2 a_{2y} + m_3 a_{3y} + m_5 a_{5y} + (m_2 + m_3 + m_5)g
 \end{aligned} \tag{5.1-10}$$

to member 2 are obtained. The torque M_{t2} at the joint can be calculated from the moment equilibrium condition. By applying the same routine to member 1, it is possible to derive expressions for the support reactions:

$$\begin{aligned}
 R_{1x} &= m_1 a_{1x} + m_2 a_{2x} + m_3 a_{3x} + m_4 a_{4x} + m_5 a_{5x}, \\
 R_{1y} &= m_1 a_{1y} + m_2 a_{2y} + m_3 a_{3y} + m_4 a_{4y} + m_5 a_{5y} + \\
 &\quad + (m_1 + m_2 + m_3 + m_4 + m_5)g
 \end{aligned} \tag{5.1-11}$$

The torque M_{t1} is obtained again from the moment equilibrium condition. Corresponding to the standard Lagrangian approach, the torques M_{t1} and M_{t2} must be the same as those computed from (5.1-7). The resulting support reactions are:

$$R_1 = \sqrt{R_{1x}^2 + R_{1y}^2}, \quad R_2 = \sqrt{R_{2x}^2 + R_{2y}^2}. \tag{5.1-12}$$

The torques M_{ti} and the forces R_i are chosen as criteria in the optimization model. It is important to present the detailed expressions for M_{ti} and R_i because the choice of the design variables as well as the general complexity of the optimization problem are associated with these formulae.

5.1.3 Formulation of the Optimization Problem

Next, a multicriteria optimization problem based on the rigid-body kinetic model of the robot arm (see Fig. 5.1/2) will be formulated, and the numerical design data for this case will be given. The objective is to find such masses m_4 and m_5 for the counterweights and such joint distances x_1 and x_2 which will minimize the chosen four design criteria. Consequently, the design variable vector is

$$\mathbf{x} = (x_1, x_2, x_3, x_4)^T, \tag{5.1-13}$$

where the first two are the distances shown in Fig. 5.1/2, $x_3 = m_4$ and $x_4 = m_5$. The upper and the lower limits for all these four design variables can be given in the form

$$x_i^l \leq x_i \leq x_i^u, \quad i = 1, \dots, 4. \tag{5.1-14}$$

The torques M_{t1} and M_{t2} at the arm joints are chosen as the first two criteria of the vector objective function. Their minimization is important because it is then possible to use smaller motors, and the energy consumption is lower if the variation ranges of the torques are small. In the explicit expressions (5.1-7), terms $m_4 x_1$, $m_4 x_1^2$, $m_5 x_2$, and $m_5 x_2^2$ appear, and thus it is reasonable to choose the design variables in the way presented.

The torques do not depend on the design variables alone but also on the position of the robot arm (θ_1, θ_2) , on the angular velocities $(\dot{\theta}_1, \dot{\theta}_2)$, and on the angular accelerations $(\ddot{\theta}_1, \ddot{\theta}_2)$. Usually, the working space of the robot arm is restricted, and thus constraints of the form

$$\theta_i^l \leq \theta_i \leq \theta_i^u, \quad i = 1, 2, \quad (5.1-15)$$

are needed. Here, θ_i^l and θ_i^u are the lower and the upper limits of the angles θ_i . In each position of the arm, the angular velocities and accelerations may be different. In order to optimize the performance of the robot, the torques should be as small as possible at all working positions and at all existing angular velocity acceleration combinations. Thus, the first two criteria are chosen as follows:

$$f_1(\mathbf{x}) = \max_{\theta_1} \max_{\theta_2} \max_{\dot{\theta}_1, \ddot{\theta}_1} M_{t1}, \quad (5.1-16)$$

$$f_2(\mathbf{x}) = \max_{\theta_1} \max_{\theta_2} \max_{\dot{\theta}_1, \ddot{\theta}_1} M_{t2},$$

where notation $\dot{\theta}_i$, $\ddot{\theta}_i$ is associated with the chosen angular velocity profile. This is shown in Fig. 5.1/4 where a trapezoidal profile, typical of robot applications, has been depicted for both members. The corresponding angular accelerations are also presented in this figure.

The construction of joints, especially the choice of bearings, depends largely on the reaction forces at the joints. Thus, it seems reasonable to choose the maximum values of the joint forces as two additional criteria. By using the fixed trapezoidal velocity profiles (see Fig. 5.1/4) and every feasible position of the arm, these criteria can be expressed in the form

$$f_3(\mathbf{x}) = \max_{\theta_1} \max_{\theta_2} \max_{\dot{\theta}_1, \ddot{\theta}_1} R_1, \quad (5.1-17)$$

$$f_4(\mathbf{x}) = \max_{\theta_1} \max_{\theta_2} \max_{\dot{\theta}_1, \ddot{\theta}_1} R_2.$$

The geometrical interpretation of all the four criteria is the following: a small movement at every position (θ_1, θ_2) of the arms is performed by using the fixed trapezoidal profiles $(\dot{\theta}_1, \dot{\theta}_2, \ddot{\theta}_1, \ddot{\theta}_2)$ shown in Fig. 5.1/4, and the maximum values of the torques and the joint forces during the movement are selected.

By using the design variables x_i given in (5.1-13), the criteria presented in (5.1-16) and (5.1-17), the side constraints of (5.1-14), and the state constraints of (5.1-15), it is now possible to formulate the multicriteria optimization problem

$$\min (f_1(\mathbf{x}), f_2(\mathbf{x}), f_3(\mathbf{x}), f_4(\mathbf{x}))^T, \quad (5.1-18)$$

subject to

$$\theta_i^l \leq \theta_i \leq \theta_i^u, \quad i = 1, 2,$$

$$x_i^l \leq x_i \leq x_i^u, \quad i = 1, 2, 3, 4.$$

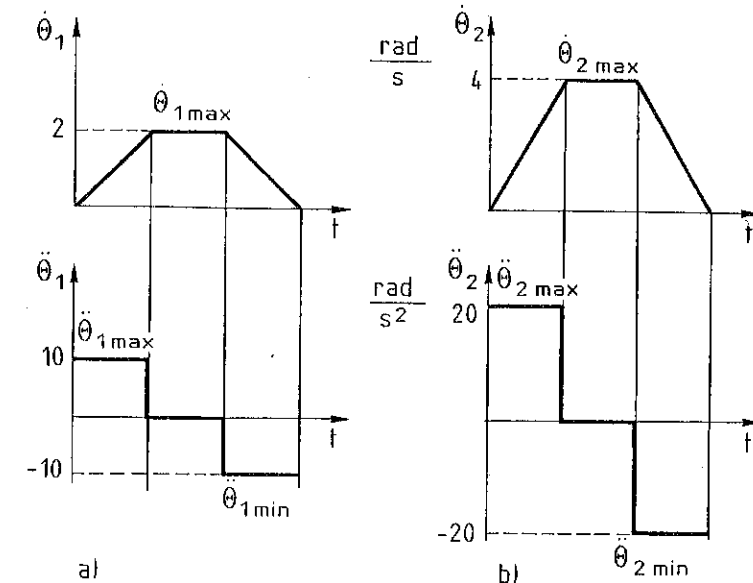


Fig. 5.1/4. Angular velocities and corresponding angular accelerations of robot arms

The minimum values of conflicting criteria cannot be obtained at the same design point. In multicriteria problems it is reasonable to apply the Pareto-optimality concept which is described in Chapter 1. Usually, not just one, but a set of Pareto-optima is characteristic of a multicriteria problem. The corresponding vectors $f(\mathbf{x}^*) = (f_1(\mathbf{x}^*), f_2(\mathbf{x}^*), f_3(\mathbf{x}^*), f_4(\mathbf{x}^*))^T$ in the criterion space R^4 are called "minimal solutions".

Next, the numerical design data for the design problem is given. These values are close to the arms of the PUMA-560 robot shown in Fig. 5.1/1 [6]. By using the notations defined in Fig. 5.1/2 and in (5.1-13), the following data are used in the optimization calculations:

$$m_1 = 17 \text{ kg}, \quad m_2 = 6 \text{ kg}, \quad m_3 = 2 \text{ kg},$$

$$L_1 = L_2 = 0.43 \text{ m}, \quad e_1 = 0.07 \text{ m}, \quad e_2 = 0.14 \text{ m},$$

$$\theta_1^l = -40^\circ, \quad \theta_1^u = 220^\circ, \quad \theta_2^l = -140^\circ, \quad \theta_2^u = 140^\circ,$$

$$\dot{\theta}_{1 \max} = 2 \frac{\text{rad}}{\text{s}}, \quad \dot{\theta}_{2 \max} = 4 \frac{\text{rad}}{\text{s}},$$

$$\ddot{\theta}_{1 \max} = 10 \frac{\text{rad}}{\text{s}^2}, \quad \ddot{\theta}_{2 \max} = 20 \frac{\text{rad}}{\text{s}^2},$$

$$x_1^l = x_2^l = 0, \quad x_1^u = x_2^u = 0.2 \text{ m}, \quad x_3^l = x_4^l = 0,$$

$$x_3^u = 35 \text{ kg}, \quad x_4^u = 15 \text{ kg},$$

$$J_1 = 0.2619 \text{ kgm}^2, \quad J_2 = 0.0924 \text{ kgm}^2.$$

5.1.4 Solution Method

The numerical solution of the robot arm balancing problem (5.1-18) is obtained on the basis of the Computer Aided Multicriteria Optimization System (CAMOS) which uses several scalar and multicriteria optimization methods (see Chapter 3 and [7]). For the problem treated here the method of combined random and sequential search has been used for the generation of Pareto-optima. The choice of the method was mainly based on the expectation of several local minima which proved to be true during the calculations. First, some points were generated by the random search method, and the best of them were stored and used as the starting points for the sequential search

procedure. By minimizing each criterion separately in the feasible set, the ideal vector $\bar{\mathbf{f}} = (\bar{f}_1, \bar{f}_2, \bar{f}_3, \bar{f}_4)^T$ was obtained. After the numerical solution of these four scalar optimization problems, it was possible to use the weighting min-max method (see (1.22)) for generating several Pareto-optimal solutions. Here, the weights w_i ($i = 1, \dots, 4$) were used as parameters which could be normalized by using $w_1 + w_2 + w_3 + w_4 = 1$. Each parameter combination corresponds to one Pareto-optimum of the problem (5.1-18). While seeking both, the ideal vector and the other Pareto-optima, the random search method was used in combination with the Nedler-Mead simplex method [8] with a penalty function.

For the numerical computation of the criteria values, the term $\max_{\theta_1}(\cdot)$ can be obtained in the following way. The value of each torque θ_1 and of each joint force is calculated at the positions $\theta_1^l, \theta_1^l + \Delta\theta_1, \theta_1^l + 2\Delta\theta_1, \dots, \theta_1^u$ where the increment $\Delta\theta_1$ is properly chosen. Then the maximum value of these positions is selected separately for each criterion. The same calculations can be carried out for the term $\max_{\theta_2}(\cdot)$ after choosing increment $\Delta\theta_2$. The smaller the increments $\Delta\theta_i$, the better the accuracy. However, the computation time is increased. The terms $\max_{\dot{\theta}_i, \ddot{\theta}_i}(\cdot)$ require the computation of torques and joint forces for all expected combinations of $\dot{\theta}_i$ and $\ddot{\theta}_i$ which is impossible to realize. Thus, only some chosen combinations of the angular velocities and accelerations are considered for given θ_1 and θ_2 . These can be found in Table 5.1/1 which presents the seven calculation points. After calculating M_{ci} and R_i for all the rows in Table 5.1/1 the maximum values can be chosen.

It is obvious that the numerical evaluation of the criteria values is computationally expensive. Using the IBM PC/AT computer, the calculation of the ideal vector $\bar{\mathbf{f}}$ needs about three hours, and the subsequent calculation of any other Pareto-optimum about one hour each. The application of the method presented in Chapter 5.2 can make the computation process more efficient. For some robot applications, the evaluation of the objective functions can be simplified by assuming for example that calculations of M_{ci} and R_i are carried out only for certain positions of the robot arms as well as for selected angular velocities and accelerations (e.g. points 3 and 5 in Table 5.1/1). Such alternatives are available when using the computer program for the presented optimization model.

Point	$\dot{\theta}_1$	$\dot{\theta}_2$	$\ddot{\theta}_1$	$\ddot{\theta}_2$
1	0	0	$\ddot{\theta}_{1\max}$	$\ddot{\theta}_{2\max}$
2	$\frac{1}{2} \dot{\theta}_{1\max}$	$\frac{1}{2} \dot{\theta}_{2\max}$	$\ddot{\theta}_{1\max}$	$\ddot{\theta}_{2\max}$
3	$\dot{\theta}_{1\max}$	$\dot{\theta}_{2\max}$	$\ddot{\theta}_{1\max}$	$\ddot{\theta}_{2\max}$
4	$\dot{\theta}_{1\max}$	$\dot{\theta}_{2\max}$	0	0
5	$\dot{\theta}_{1\max}$	$\dot{\theta}_{2\max}$	$-\ddot{\theta}_{1\max}$	$-\ddot{\theta}_{2\max}$
6	$\frac{1}{2} \dot{\theta}_{1\max}$	$\frac{1}{2} \dot{\theta}_{2\max}$	$-\ddot{\theta}_{1\max}$	$-\ddot{\theta}_{2\max}$
7	0	0	$-\ddot{\theta}_{1\max}$	$-\ddot{\theta}_{2\max}$

Table 5.1/1. Angular velocities and accelerations at the calculation points shown in Figure 5.1/4

5.1.5 Pareto-Optimal Designs

Fifteen Pareto-optimal robots have been generated by using the module of CAMOS which calculates one Pareto-optimum for each weighting coefficient combination. The weights w_i ($\sum w_i = 1$), the Pareto-optimal design variable vectors \mathbf{x}^* , and the corresponding minimal solutions \mathbf{f}^* are shown in Table 5.1/2. The results are illustrated graphically in Fig. 5.1/5 which presents four Pareto-optimal robot arms.

In Fig. 5.1/6 the minimal solutions have been presented graphically. Pareto-optima 1...15 are in such an order that criterion f_1 is increasing continuously. Thus, \mathbf{x}_i^* and \mathbf{x}_{i+1}^* are not necessarily neighbouring points in the design space. If the minimal set is represented sufficiently, it is possible to obtain a satisfactory solution, i.e. the best Pareto-optimum from this kind of a figure. Otherwise, one can apply the procedure given in CAMOS where \mathbf{w} is changed until a satisfactory solution is found.

$\mathbf{w} = (w_1, w_2, w_3, w_4)^T$	$\mathbf{x} = (x_1, x_2, x_3, x_4)^T$	$\mathbf{f}(\mathbf{x}) = (f_1(\mathbf{x}), f_2(\mathbf{x}), f_3(\mathbf{x}), f_4(\mathbf{x}))^T$	No.
$\min f_1(\mathbf{x})$	(0.199, 0.199, 34.98, 5.77)	(85.7, 32.2, 750.6, 302.8)	1
$\min f_2(\mathbf{x})$	(0.175*, 0.114, 10.24*, 14.86)	(162.7, 23.2, 711.1, 450.7)	15
$\min f_3(\mathbf{x})$	(0.198*, 0.14*, 0.001, 0.002)	(132.2, 41.9, 373.8, 194.5)	12
$\min f_4(\mathbf{x})$	(0.191*, 0.198*, 14.3*, 0.001)	(111.3, 41.9, 419.4, 194.5)	4
(0.25, 0.25, 0.25, 0.25)	(0.186, 0.198, 7.95, 4.06)	(125.5, 35.0, 509.8, 268.5)	10
(0.3, 0.3, 0.2, 0.2)	(0.171, 0.184, 16.9, 5.66)	(117.8, 32.5, 599.1, 299.1)	7
(0.35, 0.35, 0.15, 0.15)	(0.194, 0.182, 19.6, 7.59)	(114.2, 29.5, 666.9, 336.19)	6
(0.4, 0.4, 0.1, 0.1)	(0.130, 0.193, 32.9, 7.84)	(107.9, 28.6, 769.6, 345.6)	3
(0.2, 0.2, 0.3, 0.3)	(0.190, 0.197, 8.05, 3.82)	(125.0, 35.5, 505.2, 263.3)	9
(0.15, 0.15, 0.35, 0.35)	(0.126, 0.175, 3.89, 2.93)	(132.9, 37.2, 457.3, 244.8)	13
(0.1, 0.1, 0.4, 0.4)	(0.103, 0.114, 0.138, 2.08)	(138.5, 39.3, 408.9, 228.2)	14
(0.5, 0.1, 0.2, 0.2)	(0.172, 0.093, 26.5, 0.45)	(99.0, 41.4, 582.3, 201.6)	2
(0.1, 0.5, 0.2, 0.2)	(0.198, 0.157, 17.0, 7.84)	(121.9, 29.9, 645.9, 335.2)	8
(0.4, 0.2, 0.2, 0.2)	(0.148, 0.182, 20.6, 3.6)	(112.3, 36.0, 606.6, 257.9)	5
(0.2, 0.4, 0.2, 0.2)	(0.152, 0.198, 10.3, 6.6)	(127.7, 30.7, 584.8, 320.7)	11

Table 5.1/2. Pareto-optima and minimal solutions corresponding to the robot problem

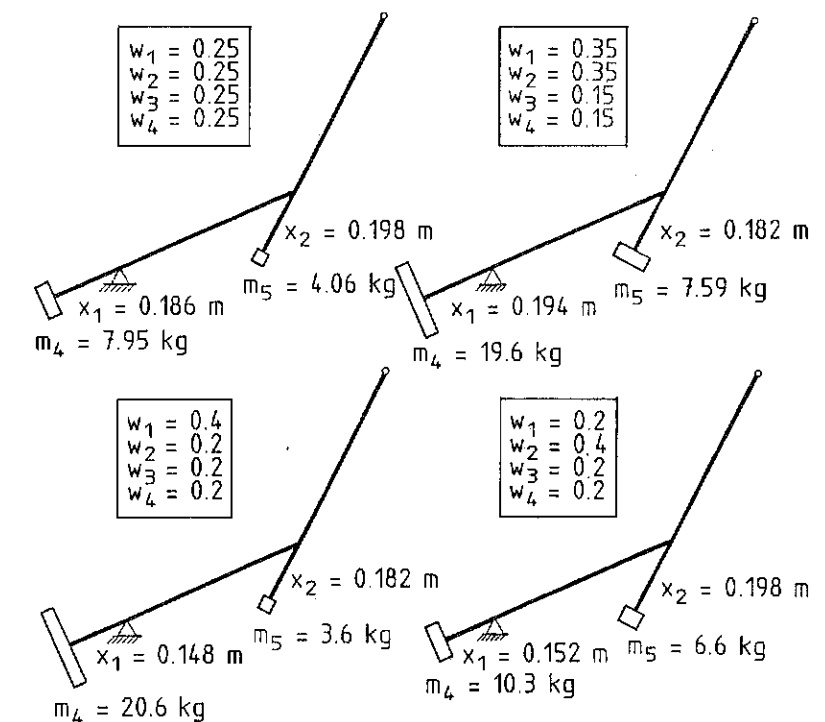


Fig. 5.1/5. Minimal solutions of Pareto-optimal robot arms

From these results it is obvious that the criteria f_1 and f_2 are in conflict with each other as well as with f_3 and f_4 . The last two criteria, however, are more or less nonconflicting. This observation suggests that a combined criterion $\lambda_1 f_3 + \lambda_2 f_4$ could be used to decrease the dimension of the multicriteria problem. Here, it is also possible to choose $\lambda_1 = 1$, $\lambda_2 = 0$, i.e. one reaction represents both. This seems reasonable also from a physical point of view. It is interesting to notice the large variation in ranges of the criteria values, even if all solutions are already Pareto-optimal. The solutions seem to be very sensitive to the design variables which are not active but located at the separately attainable minima. At these points some variables can be chosen freely, and they are depicted by an asterisk (*) in Table 5.1/2. Note that when the mass of the counterweight is close to zero, variables x_1 or x_2 do not influence the solution.

Variables x_1 and x_3 have no influence on the minimum of $f_2(\mathbf{x})$ and $f_4(\mathbf{x})$ which is the case when weak Pareto-optima occur [9]. Thus, the values of x_1 and x_3 in the rows two and four of Table 5.1/2 were obtained while additionally minimizing $f_1(\mathbf{x})$ and $f_2(\mathbf{x})$ with equal importance for the given values of x_2 and x_4 , established at the separately attainable minima of $f_3(\mathbf{x})$ and $f_4(\mathbf{x})$.

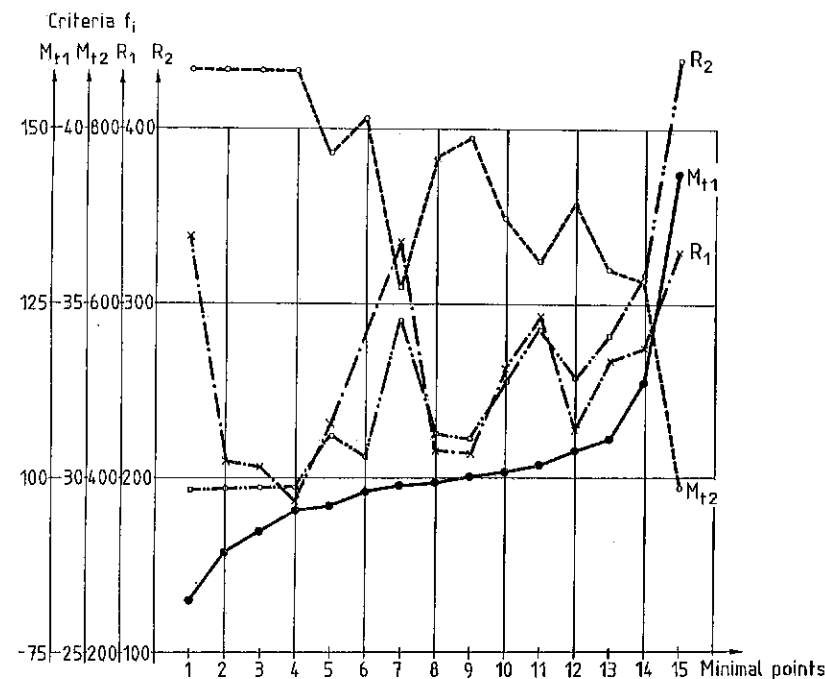


Fig. 5.1/6. Minimal solutions of the multicriteria robot problem

5.1.6 Conclusion

A multicriteria optimization problem for robot arm balancing has been formulated by using dynamic support reactions and torques as criteria. Lengths and masses of balancing mechanisms have been used as design variables, and side constraints have been applied to these variables. The mathematical solution to this problem, called the Pareto-optimal set, is represented by fifteen Pareto-optima obtained by the optimization system CAMOS. These correspond to fifteen different robot designs and points in the criterion space.

These results show that the optimal structures differ considerably depending on the importance given to each criterion. Also, the criterion values vary from one optimal solution to another. This suggests that plenty of Pareto-optima should be available for the designer who can bring in his personal experience in choosing the best available structure. The numerical computation involved is costly and time-consuming. Another problem is the probable existence of local minima in this very nonconvex problem. The results also show that it is difficult to predict the optimal mass distribution for these dynamic criteria without applying the optimization approach.

The design of robot arms is a complex problem including the aspects of strength, flexibility, and vibration. The overall optimization problem is very extensive, and thus it is difficult to solve it numerically even for one Pareto-optimum. Furthermore, the aspects associated with robot control should be considered in the design process. This will unavoidably result in the application of several criteria such as mass, energy consumption, stiffness, control index. It seems practical to proceed into a hierarchical optimization process where several subproblems such as dynamic behaviour, structural design, and control design are treated as separate problems. One subproblem is that of balancing; it can be based completely on the rigid-body motion of the arms, thus resulting in a problem of practical size and complexity. Now that a set of optimal alternatives is available to the designer, it is possible to make the structural design of the arms more flexible than if all data values were to be fixed.

The module which generates the Pareto-optima for this dynamic problem is an important part of an interactive design system. This system is under development, and sensitivity information between the subsystems will be needed to create a working computer aided design

system for robot arms. In addition to this, problems will also arise in the numerical solution of the min-max-max-max-type problem when more arms are considered and more Pareto-optima are needed.

References

- [1] Herve, I.M.: Design of Spring Mechanism for Balancing the Weight of Robots. Proceedings of the 6th Symposium of Theory and Practice of Robots and Manipulators. Cracow, Poland: MIT Press 1986
- [2] Subbiah, M.; Sharan, A.M.: The Optimal Balancing of the Robotic Manipulation. IEEE. CH2282-2 (1986) 828-835
- [3] Hockey, B.A.: The Minimization of the Fluctuation of Input Shaft Torque in Plane Mechanisms. Mechanisms and Machine Theory Vol. 7 (1972) 335-346
- [4] Lee, T.W.; Cheng, C.: Optimum Balancing of Combined Shaking Force, Shaking Moment and Torque Fluctuations in High-Speed Linkages. ASME Paper No. 83-DET-9, Design and Production Engineering. Technical Conference, September 1983
- [5] Tricano, S.J.; Lowen, G.G.: Simultaneous Optimization and Dynamic Reactions of Four-Bar Linkage with Prescribed Maximum Shaking Force. ASME Journal of Mechanisms, Transmission and Automation in Design, Vol. 105 (1983) 520-525
- [6] Armstrong, B.; Oussama, K; Burdick, J.: The Explicit Dynamic Model and Inertial Parameters of the PUMA 560 Arm. IEEE (1986) 510-521
- [7] Osyczka, A.: Computer Aided Multicriterion Optimization System (CAMOS). In: Proceedings of a GAMM-Seminar, October 5-7, 1988, Siegen, FRG, Berlin, Heidelberg, New York, London, Paris, Tokyo 1989
- [8] Nelder, J.A.; Mead, R.A.: Simplex Method for Function Minimization. Computer J., Vol. 7 (1965) 308-313
- [9] Koski, J.: Bicriterion Optimum Design Method for Elastic Trusses. Dissertation. Acta Polytechnica Scandinavica, Mechanical Engineering Series No. 86, Helsinki 1984

Appendix

The terms appearing in the condensed equation (5.1-7) are:

Coefficients for torque M_{t1} :

$$D_{11} = m_1 e_1^2 + m_4 x_1^2 + m_2 e_2^2 + m_3 L_2^2 + m_5 x_2^2 + (m_2 + m_3 + m_5) L_1^2 + 2m_2 e_2 L_1 \cos \theta_2 + 2m_3 L_1 L_2 \cos \theta_2 - 2m_5 x_2 L_1 \cos \theta_2 + J_1 + J_2,$$

$$D_{12} = m_2 e_2^2 + m_3 L_2^2 + m_5 x_2^2 + m_2 e_2 L_1 \cos \theta_2 + m_3 L_1 L_2 \cos \theta_2 - m_5 x_2 L_1 \cos \theta_2 + J_2,$$

$$D_{11}^1 = -m_5 x_2 L_1 [\sin(\theta_0 + \theta_1) + \sin \theta_2] + m_5 x_2^2 \sin 2\theta_0,$$

$$D_{12}^2 = -m_2 e_2 L_1 \sin \theta_2 - m_3 L_1 L_2 \sin \theta_2 - m_5 x_2 L_1 \sin(\theta_0 + \theta_1) + m_5 x_2^2 \sin 2\theta_0,$$

$$D_{12}^1 + D_{11}^2 = -2m_2 e_2 L_1 \sin \theta_2 - 2m_3 L_1 L_2 \sin \theta_2 - 2m_5 x_2 L_1 \sin(\theta_0 + \theta_1) + 2m_5 x_2^2 \sin 2\theta_0,$$

$$D_1 = m_1 g e_1 \cos \theta_1 - m_4 g x_1 \cos \theta_1 + m_2 g e_2 \cos \theta_0 + m_3 g L_2 \cos \theta_0 - m_5 g x_2 \cos \theta_0 + (m_2 + m_3 + m_5) g L_1 \cos \theta_1.$$

Coefficients for torque M_{t2} :

$$D_{21} = m_2 (L_1 e_2 \cos \theta_2 + e_2^2) + m_3 (L_1 L_2 \cos \theta_2 + L_2^2) - m_5 (L_1 x_2 \cos \theta_2 - x_2^2) + J_2,$$

$$D_{22} = m_2 e_2^2 + m_3 L_2^2 + m_5 x_2^2 + J_2,$$

$$D_{21}^1 = m_2 L_1 e_2 \sin \theta_2 + m_3 L_1 L_2 \sin \theta_2 + m_5 (2x_2^2 \sin \theta_0 \cos \theta_0 - L_1 x_2 \sin \theta_2),$$

$$D_{22}^2 = 2m_5 x_2^2 \sin \theta_0 \cos \theta_0,$$

$$D_{22}^1 + D_{21}^2 = 4m_5 x_2^2 \sin \theta_0 \cos \theta_0,$$

$$D_2 = m_2 g e_2 \cos \theta_0 + m_3 g L_2 \cos \theta_0 - m_5 g x_2 \cos \theta_0,$$

where J_1 and J_2 are the rotary inertias of members 1 and 2, respectively. Notation $\theta_0 = \theta_1 + \theta_2$ is used for convenience.